PARAMETERS ANALYSIS CHARACTERIZING THE ELEMENT FREE GALERKIN METHOD

Flávia Romano Villa Verde, flaviarvv@unb.br
Gerson Henrique Pfitscher, gerson@unb.br
Dianne Magalhães Viana, diannemv@unb.br
Jorge Luiz Ferreira de Almeida, jorge@unb.br
Universidade de Brasília, Campus Darcy Ribeiro, Brasília, DF, Brazil

Abstract. *The Finite Element Method is well established for modeling complex problems in applied mechanics and related fields. However, in several classes of problems, the mesh generation may lead to additional costs. To prevent this drawback, numerical techniques have been developed in such a way that the mesh is not more necessary to discretize the problem. In these methods, called meshless or meshfree, the trial functions are constructed entirely in terms of a set of nodes without the necessity of element discretization for the construction of the equations. The ideal requirement for a method be considered meshless is that the mesh structure be completelly eliminated from the problem solution process, but considering the minimum requirement, it is sufficient that the mesh be dispensable in field variable interpolation. Element Free Galerkin method (EFG) is one of the most interesting type of meshless methods. Although it is considered meshless, the EFG utilizes a background mesh to assembly the equations system that describes the problem. To implement this technique, it is necessary to characterize the following parameters: I) influence domain, II) weight function, III) number of cells, and IV) number of nodes. The goal of this work is to verify the influence of these parameters in the numerical model results. This will be done by comparing the displacement and stress fields obtained by the EFG method for different combinations of the parameters related above with the respective analytic solution of the stress analysis problem.*

Keywords*: meshless methods, Element Free Galerkin, stress analysis.*

1. INTRODUCTION

Some problems of practical importance are handled through conventional methods like finite elements, finite differences, and finite volumes. However these methods can present many difficulties and be computationally expensive for certain classes of problems such as crack propagation, problems with phase change, large-strain deformations, etc, for the fact these methods are related to meshes. Meshless methods appear as an attractive alternative for analyzes of these classes of problems (Duarte, 1995).

Meshless methods are used to establish systems of algebraic equations for the domain altogether of a problem without a predefined mesh. These methods operate with a set of distributed points inside the domain Ω as well as with sets of points distributed on its boundary to represent (but not discretize) the domain of the problem and its boundary. This set of distributed points does not generate a mesh, meaning that it is not required any information about the relations between these points (Liu, 2004) (Belytschko et al, 1996).

The minimum requirement for a method to be considered meshfree is that it is not necessary a predefined mesh, at least in the interpolation of the field variables. The ideal requirement for a meshfree method is that no mesh is necessary during the whole solution process of the problem for an arbitrary geometry governed by a system of partial differential equations, for all kind of boundary conditions employed (Liu, 2004).

This work presents some results obtained with the simulation of Timoshenko's beam modeled by the Element Free Galerkin (EFG) method. Analyses are made on the effect of the parameters associated to the formulation of the EFG in the response of the model, through graphical output of the displacement fields and of normal and shear stress fields as well as through the computation of the norm of the error relative to the analytical solution. Among these parameters we have: domain of influence, weight functions, number of cells and number of points in the domain.

2. ELEMENT FREE GALERKIN

The main characteristic of the EFG method is the use of an auxiliary mesh composed only of quadrature elements that completely cover the domain of the analyzed problem. The Element Free Galerkin method proposed by Belytschko et al (1994) is based on the diffuse element method developed by Nayroles et al (1992). In Element Free Galerkin method only a set of points and the description of the model of boundaries are necessary to generate the discrete equations. The connectivity among points and the trial functions are completely built by the method. Although the EFG method be considered a meshfree method when it relates to the construction of the shape function or function approximation, a mesh is necessary to construct the partial differential equations by the Galerkin approximation procedure (Dolbow and Belytschko, 1998). The EFG method is based on the Moving Least Square Method (MLSM) to approximate a function $u(\mathbf{x})$ to $u^h(\mathbf{x})$ in a domain Ω using a set of nodal points x_I, $I = 1..n_t$, to formulate the discrete model (Belytschko, 1996). These approximations are built up from three elements: (i) a weight function with a compact support, associated to each nodal point, (ii) a polynomial basis, and (iii) a set of coefficients depending on its coordinates. The MLSM is an approximation based on the weighted least squares, with a weight function w moving to the interpolation point $\mathbf{x}$. An important property of the MLSM is its consistency of order k, where k is the degree of the highest order of the basis $p(\mathbf{x})$. For k = 0 (zero order consistency) the concept of partition-of-unity is also satisfied by the MLSM.

2.1. System of equations

Consider the function $u(\mathbf{x})$ of a field variable defined in the domain Ω. An approximation of $u(\mathbf{x})$ in the nodal point $\mathbf{x}$ is designated as $u^h(\mathbf{x})$. The first approximation by the MLSM has the form:

$$u(\mathbf{x}) \cong u^{\mathrm{h}}(\mathbf{x}) = \sum_{j}^{m} p_j(\mathbf{x}) a_j(\mathbf{x}) = \mathrm{p}^{\mathrm{T}}(\mathbf{x}) \cdot \mathbf{a}(\mathbf{x}) \tag{1}$$

where $\mathbf{p}$ is a vector storing monomials, m is the number of monomial terms, and $\mathbf{a}$ the vector of coefficients:

$$\mathbf{p}^{\mathrm{T}}(\mathbf{x}) = [1 \quad x \quad x^2 \ \dots \ x^m], \quad \text{and} \quad \mathbf{a}^{\mathrm{T}}(\mathbf{x}) = [a_0 \quad a_1 \quad a_2 \ \dots \ a_m]. \tag{2}$$

The coefficients $\mathbf{a}(\mathbf{x})$ are obtained by minimizing the quadratic functional J. The functional of a weighted residual is obtained using the approximate values of the function field and the nodal parameters $u_I = u(x_I)$. J is given by

$$J = \sum_{\mathrm{I}}^{\mathrm{n}} \mathrm{w}\left(\mathbf{x} - \mathbf{x}_{\mathrm{I}}\right)\left[\mathbf{p}(\mathbf{x}_{\mathrm{I}}) \cdot \mathbf{a}(\mathbf{x}) - \mathrm{u}_{\mathrm{I}}\right]^2 \quad \text{or} \quad J = \left[\mathbf{P} \cdot \mathbf{a} - \mathbf{U}\right]^{\mathrm{T}} \cdot \mathbf{W}\left(\mathbf{x}\right) \cdot \left[\mathbf{P} \cdot \mathbf{a} - \mathbf{U}\right] \tag{3}$$

where $w(\mathbf{x}-\mathbf{x}_I)$ is the weight function. The $\mathbf{P}$ matrix has the dimension of the number of terms of the monomial base m multiplied by the number of nodes in the influence domain n. The diagonal matrix $\mathbf{W}$ stores the weight function values $w(\mathbf{x}-\mathbf{x}_I)$. For the two-dimensional linear base (m = 3) we have

$$\mathbf{P} = \begin{bmatrix} 1 & 1 & \dots & 1 \\ \mathrm{x}_1 & \mathrm{x}_2 & \cdots & \mathrm{x}_n \\ \mathrm{y}_1 & \mathrm{y}_2 & \dots & \mathrm{y}_n \end{bmatrix}, \quad \text{and} \quad \mathbf{W}(\mathbf{x}) = \begin{bmatrix} \mathrm{w}(\mathrm{x}-\mathrm{x}_1) & 0 & \dots & 0 \\ 0 & \mathrm{w}(\mathrm{x}-\mathrm{x}_2) & \cdots & 0 \\ 0 & 0 & \dots & \mathrm{w}(\mathrm{x}-\mathrm{x}_n) \end{bmatrix} \tag{4}$$

where x_I e y_I are the nodes spatial coordinates that belong to the influence domain analyzed. The minimization of the quadratic functional J, $\partial J/\partial a = 0$, gives:

$$\mathbf{A}(\mathbf{x}) \cdot \mathbf{a}(\mathbf{x}) = \mathbf{B'}(\mathbf{x}) \cdot \mathbf{U} \tag{5}$$

The vector $\mathbf{U}$ stores the nodal parameters for the field variables analyzed for all nodes of the influence domain, being $\mathbf{A}$, the moment matrix, and $\mathbf{B'}$ given by:

$$\mathbf{A(x)} = \mathbf{P}^{\mathrm{T}} \times \mathbf{W(x)} \times \mathbf{P} \quad \text{and} \quad \mathbf{B'(x)} = \mathbf{P}^{\mathrm{T}} \times \mathbf{W(x)} \tag{6}$$

Isolating $\mathbf{a}$ in Eq. (5), and substituting it in Eq. (1), we can define the shape function ϕ as:

$$\boldsymbol{\phi}(\mathbf{x}) = \mathbf{p}^{\mathrm{T}}(\mathbf{x}) \cdot \mathbf{A}^{-1}(\mathbf{x}) \cdot \mathbf{B'}(\mathbf{x}) \tag{7}$$

Equation (1) can be rewritten into the form:

$$\boldsymbol{u}^{\mathrm{h}} = \begin{bmatrix} u \\ v \end{bmatrix}^{\mathrm{h}} = \sum_{\mathrm{I}}^{\mathrm{n}} \underbrace{\begin{bmatrix} \phi_{\mathrm{I}} & 0 \\ 0 & \phi_{\mathrm{I}} \end{bmatrix}}_{\boldsymbol{\Phi}_{\mathrm{I}}} \underbrace{\begin{bmatrix} u_{\mathrm{I}} \\ v_{\mathrm{I}} \end{bmatrix}}_{\mathbf{u}_{\mathrm{I}}} = \sum_{\mathrm{I}}^{\mathrm{n}} \boldsymbol{\Phi}_{\mathrm{I}} \cdot \mathbf{u}_{\mathrm{I}} \tag{8}$$

The discrete equation system is obtained by imposition of boundary conditions using Lagrange's multipliers in a weak form of a problem of linear elasticity and by making use of the approximation equations for field variables:

$$\begin{bmatrix} \mathbf{K} & \mathbf{G} \\ \mathbf{G}^{\mathrm{T}} & \mathbf{0} \end{bmatrix} \cdot \begin{bmatrix} \mathbf{u} \\ \boldsymbol{\lambda} \end{bmatrix} = \begin{bmatrix} \mathbf{f} \\ \mathbf{q} \end{bmatrix} \tag{9}$$

where $\mathbf{K}$ is the stiffness matrix, $\mathbf{G}$ is the boundary condition matrix, $\mathbf{u}$ is the nodal displacements vector, $\boldsymbol{\lambda}$ are the Lagrange multipliers, $\mathbf{f}$ is the force vector and $\mathbf{q}$ is a boundary condition vector, and

$$\mathbf{K}_{IJ} = \int_{\Omega} \mathbf{B}_I^{\mathrm{T}} \cdot \mathbf{D} \cdot \mathbf{B}_J \, d\Omega \tag{10}$$

$$\mathbf{G}_{IJ} = -\int_{\Gamma_u} \mathbf{\Phi}_I \cdot \mathbf{N}_J \, d\Gamma \tag{11}$$

$$\mathbf{f}_I = \int_{\Omega} \mathbf{\Phi}_I^{\mathrm{T}} \cdot \mathbf{b} \, d\Omega + \int_{\Gamma_t} \mathbf{\Phi}_I^{\mathrm{T}} \cdot \mathbf{t} \, d\Gamma \tag{12}$$

$$\mathbf{q}_I = -\int_{\Gamma_u} \mathbf{N}_I^{\mathrm{T}} \cdot \bar{\mathbf{u}} \, d\Gamma \tag{13}$$

where $\mathbf{N}$ is the Lagrange's interpolating polynomial matrix, $\mathbf{D}$ is an elasticity matrix for the state of plain stress, matrix $\mathbf{B}$ stores the shape function derivates, $\mathbf{b}$ is a body forces vector and $\mathbf{t}$ is a superficial forces vector In the two-dimensional case we have:

$$\mathbf{B}_I = \begin{bmatrix} \phi_{I,x} & 0 \\ 0 & \phi_{I,y} \\ \phi_{I,y} & \phi_{I,x} \end{bmatrix}, \text{ and } \quad \mathbf{N}_I = \begin{bmatrix} N_I & 0 \\ 0 & N_I \end{bmatrix} \tag{14}$$

2.2. Weight functions

A common characteristic of all meshfree methods is the weight function, defined as not null only in a small neighborhood of $\mathbf{x}_I$, called domain of influence of the nodal point, which is a subdomain $\Delta\Omega_I$, where a specific point contributes to the approximation to generate a set of sparse discrete equations, i.e. the weight function has a compact support. The supports more used are rectangles and circles. The overlapping of influence domains define the connectivities among points (Dolbow and Belytschko, 1998) (Belytschko et al, 1996).

The choice of the weight function affects the results of the approximation function u^h. When considering the one-dimensional case, $d_I = \| x - x_I \|$, and $r = d_I / d_{mI}$, where d_{mI} is the size of the influence domain of the I*th* point, the weight function can be written as a function of the standardized length r. The most used weight functions are: cubic spline (Eq. (15), Belytschko et al,1996); quartic spline (Eq. (16), Belytschko et al,1996); fifth order spline (Eq. (17), Xiaofei, 2004); Exponential1, Exp1 (Eq. (18), Belytschko,1996); Exponential2, Exp2 (Eq. (19), Shuyao, 2003); Gaussian (Eq. (20), Belytschko et al,1994) and conic (Eq. (21), Belytschko et al,1994).

$$w(x - x_I) \equiv w(r) = \begin{cases} \dfrac{2}{3} - 4r^2 + 4r^3 & \text{para } r \le \dfrac{1}{2} \\ \dfrac{4}{3} - 4r + 4r^2 - \dfrac{4}{3} r^3 & \text{para } \dfrac{1}{2} < r \le 1 \\ 0 & \text{para } r > 1 \end{cases} \tag{15}$$

$$w(x - x_I) \equiv w(r) = \begin{cases} \dfrac{2}{3} - 6r^2 + 8r^3 - \dfrac{4}{3} r^4 & \text{para } r \le 1 \\ 0 & \text{para } r > 1 \end{cases} \tag{16}$$

$$w(x-x_I) \equiv w(r) = \begin{cases} 1-10r^2+20r^3-15r^4+4r^5 & \text{para } r \le 1 \\ 0 & \text{para } r > 1 \end{cases} \tag{17}$$

$$w(x-x_I) \equiv w(r) = \begin{cases} e^{-(r/\alpha)^2} & \text{para } r \le 1 \\ 0 & \text{para } r > 1 \end{cases} \tag{18}$$

$$w(x-x_I) \equiv w(r) = \begin{cases} e^{-(r/\alpha)} & \text{para } r \le 1 \\ 0 & \text{para } r > 1 \end{cases} \tag{19}$$

$$w(x-x_I) \equiv w(r) = \begin{cases} \dfrac{e^{-(\beta r)^{2k}} - e^{-(\beta)^{2k}}}{\left(1-e^{-(\beta)^{2k}}\right)} & \text{para } r \le 1 \\ 0 & \text{para } r > 1 \end{cases} \tag{20}$$

$$w(x-x_I) \equiv w(r) = \begin{cases} 1-r^{2k} & \text{para } r \le 1 \\ 0 & \text{para } r > 1 \end{cases} \tag{21}$$

where α, β and k are weight function parameters. The weight function in the two-dimensional case for any nodal point can be written as:

$$w(x\text{-}x_I) = w(r_x) \cdot w(r_y) = w_x \, . \, w_y \tag{22}$$

where $w(r_x)$ or $w(r_y)$ is obtained by substitution of r by r_x or r_y , respectively, in the weight functions given by Eq.(15) to Eq. (21). The values of r_x and r_y are calculated by:

$$r_x = \frac{\|x-x_I\|}{d_{mx}} \quad \text{and} \quad r_y = \frac{\|y-y_I\|}{d_{my}} \tag{23}$$

The size of the influence domain d_{mI}, is given by:

$$d_{mx} = d_{max} \, . \, c_{xI} \quad \text{and} \quad d_{my} = d_{max} \, . \, c_{yI} \tag{24}$$

where c_{xI} e c_{yI} are the distance between a particular nodal point and the k-th closest points, and d_{max} is a scale factor. If the nodal points are uniformly distributed, c_{xI} and c_{yI} are the distances between points in x e y directions, respectively.

3. CASE STUDY

The problem studied deals with a cantilever beam with length L, width D and unit height, subjected to a concentrated load, P, at its free end, as represented in Fig. 1:

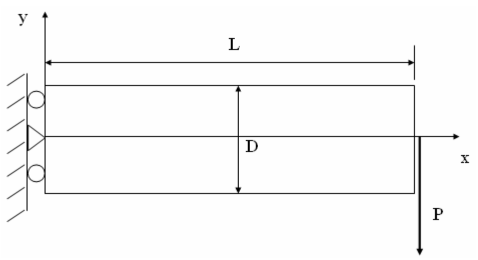

Figure 1. Cantilever beam with bending load applied at its free end (Timoshenko's beam)

Timoshenko and Goodier (1970) had considered the solution for a state of plain stress. The expressions for displacements in x direction, u_x, and in y direction, u_y, are respectively:

$$u_x = -\frac{Py}{6EI_m}\left[\left(6L-3x\right)x+\left(2+\nu\right)\left(y^2-\frac{D^2}{4}\right)\right] \tag{25}$$

$$u_y = -\frac{P}{6EI_m}\left[3\nu y^2\left(L-x\right)+\left(4+5\nu\right)\frac{D^2 x}{4}+\left(3L-x\right)x^2\right]. \tag{26}$$

P is the maximum load applied, E is the modulus of elasticity, x and y are the coordinates in x axis and y axis for the analyzed nodal point and I_m is the inertial moment, $I_m = D^3/12$. The stresses are given by:

$$\sigma_x = -\frac{P(L-x)y}{I_m} \qquad \sigma_y = 0 \qquad \sigma_{xy} = -\frac{P}{2I_m}\left(\frac{D^2}{4}-y^2\right) \tag{27}$$

4. NUMERICAL RESULTS

The numerical results presented in this section allow an analysis of the response of the EFG method in relation to its parameters. Among these related parameters they are the size of the influence domain, the weight function used, the number of points in the domain, etc. The energy norm and the relative error norm for any field variable a, Eq. (28) and Eq. (29), respectively, are used to check the error generated by the method. The results are classified into three cases. Each of them allows the evaluation of some parameters pertinent to the method. All the results presented on this section are relative to a beam with a dimension of 48×12 units of length as indicated in Fig. 1. Four points of Gauss were used in each one of the directions in the numerical integration. The interpolating polynomial used on the shape function is linear and the solution to the Eq. (9) is obtained by the LU direct method.

$$energy\ norm = \left(\frac{1}{2}\int_0^1 \left(\varepsilon_{num}-\varepsilon_{exact}\right)^T D\left(\varepsilon_{num}-\varepsilon_{exact}\right)dx\right)^{1/2} \tag{28}$$

$$La = \frac{\sqrt{\int_\Omega \left(a_{num}-a_{exact}\right)^T \cdot \left(a_{num}-a_{exact}\right)d\Omega}}{\sqrt{\int_\Omega a_{exact}^T \cdot a_{exact}\, d\Omega}} \times 100\,(\%) \tag{29}$$

where ε is a strain.

4.1. Case 1: validation

The first case was used to validate the program written in the C language. A comparison is made with the numerical values obtained and the analytical solution of the Timoshenko's beam for stress fields and displacements. We consider a beam with 55 points uniformly distributed (11×5), 40 cells of background integration (Fig. 2a), and rectangular influence domain with d_{max} equal to 3.5, c_{xI} and c_{yI} constants and equal to the length and height of the integration cells, respectively. The weight function used is the cubic spline, Eq. (15). The parameters cited above and used for validation were obtained from Dolbow and Belytschko, (1998), since they present acceptable results for the same problem.

Figures 2b, 2c and 2d show the displacement fields in y direction, normal and shear stresses fields on the 55 points of the domain, respectively. Figure 2 gives a better qualitative and quantitative understanding of the numerical values obtained for the domain.

Figure 3 shows the comparison between the analytical values of shear stress, Eq. (27), and the values obtained on Gauss's sample point in three sections of the beam. The weight functions used was the cubic spline (Fig. 3a) and the quartic spline (Fig. 3b).

Table 1 shows the error calculated using the energy norm for the two spline functions tested for the domain points and Gauss's sample points. These errors are relatively small, hence the response given by the program is close to the exact solution. The results shown are better for the cubic spline function than for the quartic spline. This can be due to the fact that the value of d_{max} proposed by Dolbow and Belytscho, (1998) is more specifically related to the cubic spline weight function tested by them.

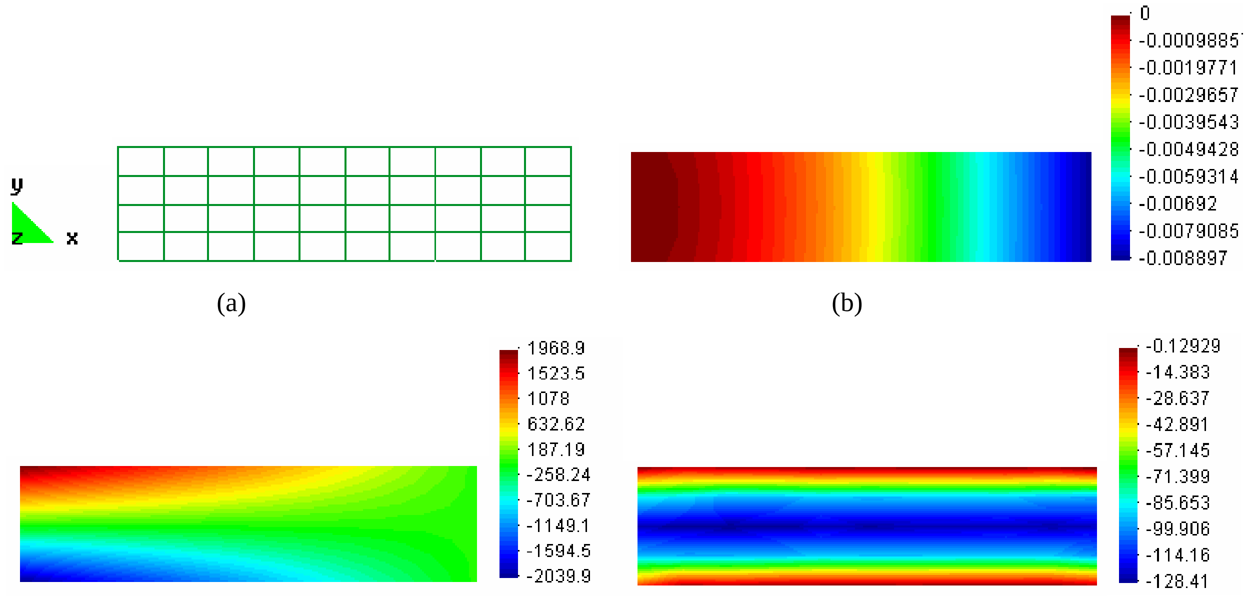

(a) (b)

(c) (d)

Figure 2. (a) background mesh; (b) displacement field in *y* direction; (c) normal stress field; and (d) shear stress field

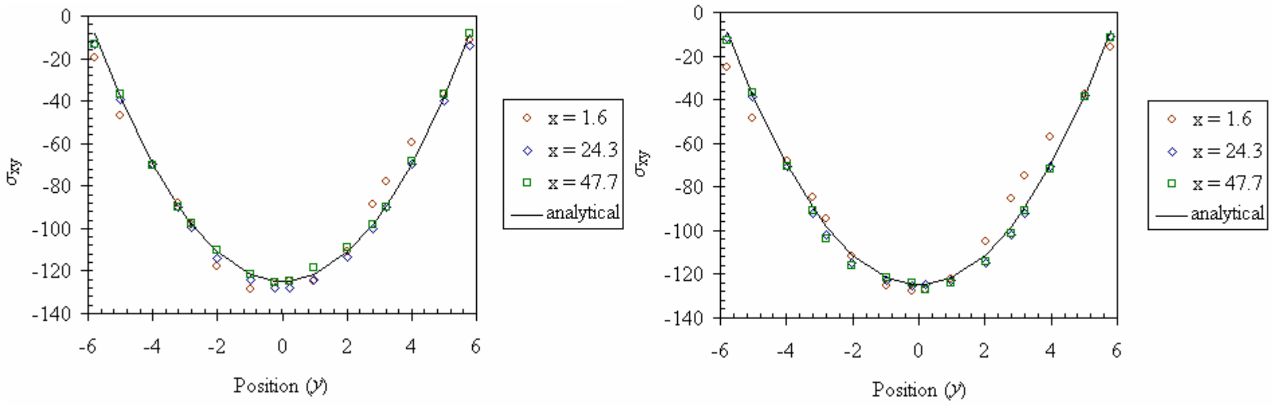

(a) (b)

Figure 3. (a) Values of analytical and numerical shear stress for three sections of the beam for the cubic spline and (b) quartic spline weight functions

Table 1. Error computed by energy norm for a rectangular domain, with d_{max} = 3.5.

Computed at	Energy norm	
	Cubic spline	Quartic spline
Sample Gauss points	0.026291	0.030096
Points of domain	0.007730	0.012441

4.2. Case 2: weight function influence

To verify the influence of the weight function on the model response, we tested seven weight functions represented by Eq. 15 to Eq. 21. The two exponential functions were evaluated for five values of α (from 0.1 up to 0.5). The Gaussian weight function was computed for five values of β, i.e. {2.0, 2.5, 3.0, 3.5, 4.0}, maintaining k = 1. The conic function was tested for k = 0.5 (linear) and k = 1.0 (second order). In this section we present the norms of the relative errors of displacement in the *y* direction, normal stress, and shear stress for two point and cell configurations of the beam represented in Fig. 1. The first configuration is the same represented in Fig.2a, 11x5 points uniformly distributed, d_{max} = 1, dm = {6..30}. The second one is formed by 85 uniformly distributed points and 64 integration cells. Fig. 4 shows the error obtained for the best responses of the tested weight functions, according to the size of the support, *dm*. Figures 4a, 4b and 4c show the errors of the first configuration and Figs. 4d, 4e and 4f for the second one.

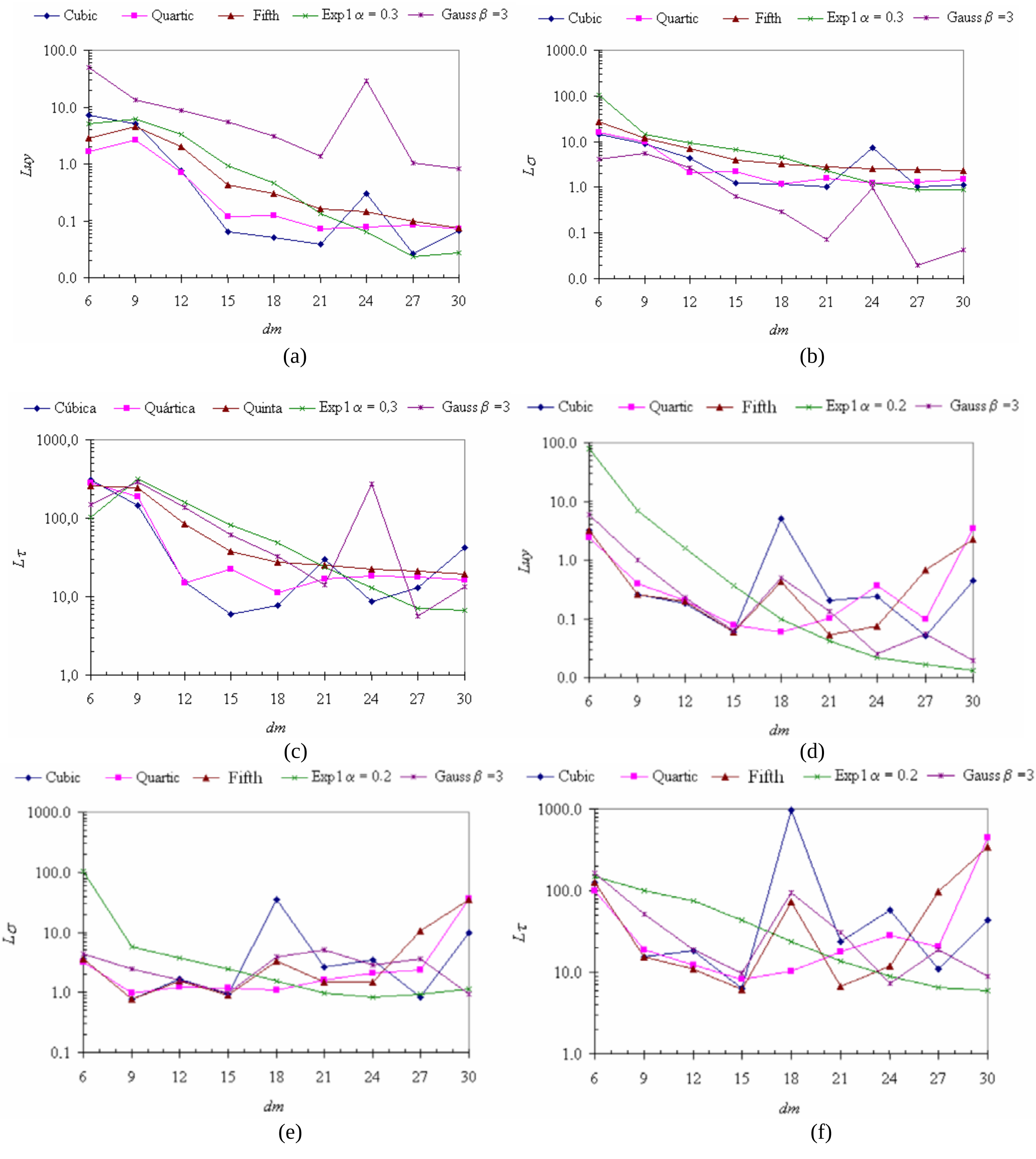

Figure 4. Relative error norm in function of *dm* for: *y* displacements (*Luy*), normal stress ($L\sigma$), shear stress ($L\tau$). Figs. 4a, 4b, and 4c show the values for 55 points and Figs. 4d, 4e, and 4f for 85 points

The size of the support *r* of the weight function associated to the desired point must be chosen big enough so that the number of points covered by the influence domain guarantee the regularity of **A**. Very small values can generate big errors when numerical integration based on Gaussian quadrature is used to calculate the array elements of the matrix. On the other hand, *r* should be small enough to maintain the local characteristics for the approximation by MLSM (Shuyao, 2003). The choice of the adjustment parameter α is of great relevance when using the exponential functions. For small values of α, the exponential weight function Exp1 presents some problems in the assembly of the matrix **A**, caused by the accentuated decay of the exponential. The exponential weight function Exp2 presents high percentage errors for shear stress in both configurations for all the tested values of α. On the other hand the Exp1 function presents very satisfactory results for some values of α.

The Gaussian function presents very similar errors for the three fields, but the scale where the error varies is higher for stress, specially shearing. The minimum errors for the β coefficients tested are similar for the two configurations, but the absolute minimum error is obtained for different values of *dm*. Small variations of *dm* produce big variations on the percentage error of the model. The response to the linear conic function (k = 0.5) is superior to the second order one (k = 1.0), however, the error associated to the shear stress field is very high for both conics tested (not shown).

The spline functions produce good results for all fields in the two configurations. Small variations in *dm* produce great variations in the percentage of the error. Table 2 indicates the range values of *dm* that the relative error diminishes, and the amount of points associated to these conditions. The range values of smaller errors are different for the two cases. However, it can be verified that the number of points associated to the size of the domain of influence presents similar values for both configurations. The use of d_{max} allows the determination of the desired number of points for several uniform configurations of points without the direct use of the parameter *dm*.

Table 2. Average, maximum and minimum number of points inside the influence domains of the sample Gauss points in the integration of the stiffness matrix **K**.

Weight function	Cubic spline		Quartic spline		Fifth order spline	
Nº of points	*dm* range for 55 nodes		*dm* range for 55 nodes		*dm* range for 55 nodes	
	dm = 15	*dm* = 21	*dm* = 12	*dm* = 24	*dm* = 15	*dm* = 30
Average	28.7	32.2	23.0	40.0	28.7	46.0
Maximum	35	40	25	50	35	55
Minimum	20	20	15	30	20	35
Nº of points	*dm* range for 85 nodes		*dm* range for 85 nodes		*dm* range for 85 nodes	
	dm = 9	*dm* = 15	*dm* = 9	*dm* = 18	*dm* = 9	*dm* = 15
Average	25.3	43.7	25.3	50.6	25.3	43.7
Maximum	30	50	30	60	30	50
Minimum	16	30	16	35	16	30

4.3. Case3: Variation of size of influence domain, *dm*

In the two previous cases the values of *dm* were fixed during all execution, that is, the influence domains had the same size. The value of *dm* can be kept fixed in cases where the distribution of points is uniform, The value of *dm* can be kept fixed in cases where the distribution of points is uniform, since knowing the rate of points distribution in the space a value of *dm* can be determined where the condition of the minimum number of points by influence domain can be satisfied. In non uniform distribution cases the k points closer to the point i of integration must be looked for and then determine the value of *dm* for i. We present the results of simulations made for the configuration with 64 cells and 85 points. c_{xI} and c_{yI} are calculated for the k nearest points. k was kept equal to 12 and d_{max} varied from 1.0 up to 3.5. The weight functions used are the cubic and quartic spline.

Figures 5a, 5b, and 6a present the percentage of error of the displacement field and stress for the tested cases. Figure 6b shows the average, maximum and minimum number of points contained in the influence domain of the sample Gauss points for the integration of the stiffness matrix. The number of points satisfying the minimum error for case 2 (constant *dm*) with 85 points, approximate to d_{max} = 1.5 for the cubical spline function and d_{max} = {1.5 .. 2.0} for the quartic spline function. It is verified that the error associated to the shear stress is very high, even for the intervals of d_{max} where a better response was expected for the model.

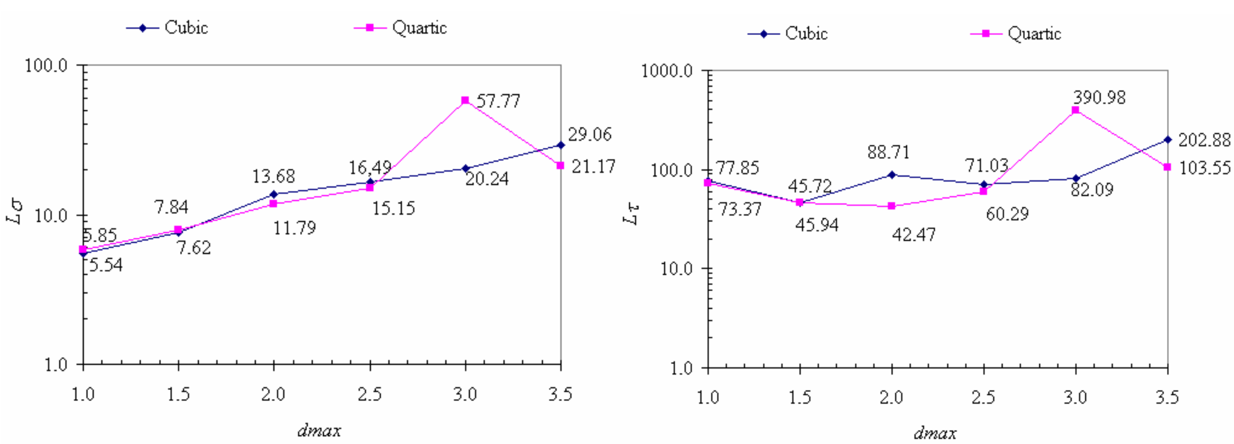

(a) (b)

Figure 5. (a) Percentage error for normal stress and (b) shear stress, for k = 12 and 85 points

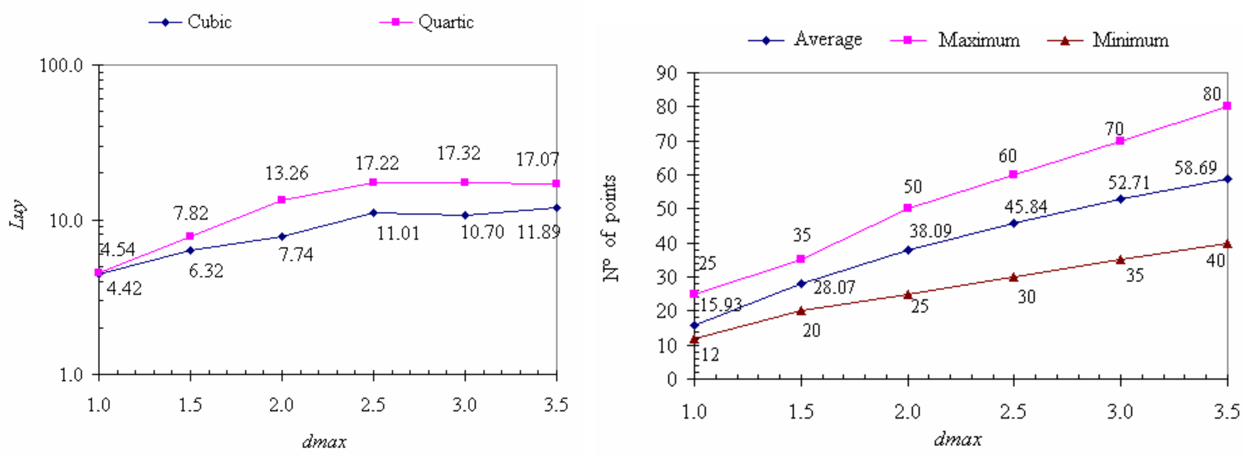

(a) (b)

Figure 6. (a) Percentage error for *y* displacements, (b) the average, maximum and minimum number of points contained in the influence domain of the sample Gauss points for the integration of the stiffness matrix

Figure 7 represents the responses for the cubic and quartic spline weight functions for normal and shear stress and for the displacement field obtained in the y direction for $d_{max} = 1.5$. Table 3 shows the average, maximum and minimum number of points inside the influence domain of the sample Gauss points in the integration of the stiffness matrix **K.**

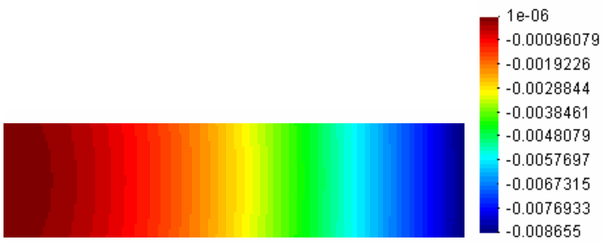

(a)

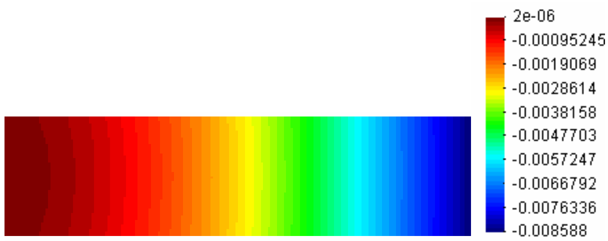

(b)

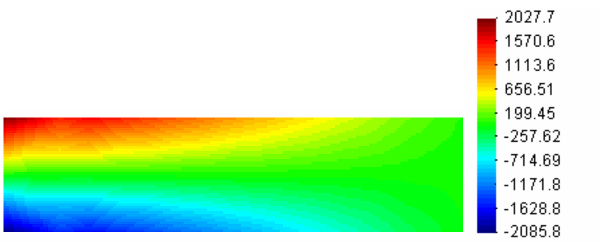

(c)

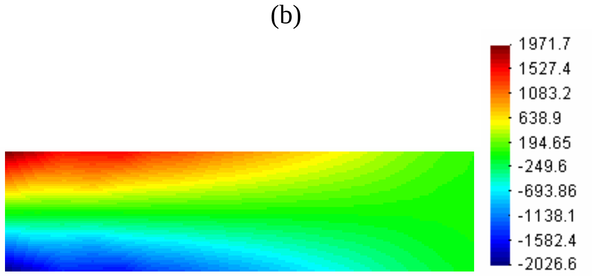

(d)

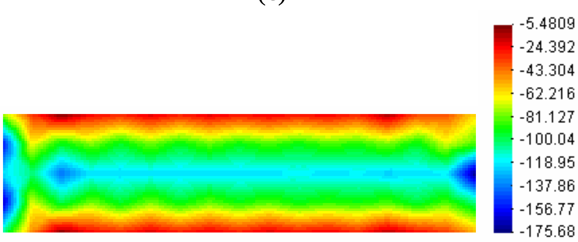

(e)

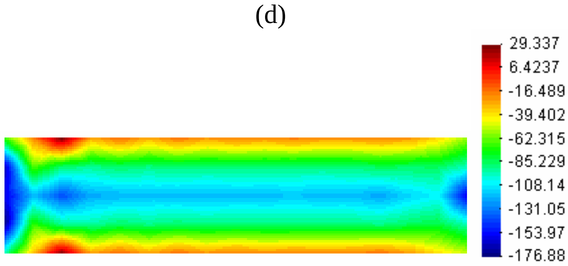

(f)

Figure 7. Displacements in *y* direction, normal stress, and shear stress fields are shown in (a), (c), and (e), respectively, for the cubic spline weight function and (b), (d) and (f) for quartic spline weight function

Table 3 shows that in all cases the minimum value for *dm* corresponds to 58.5% of the maximum value. Points belonging to the influence domains are located on the vertices of the integration cells. The distribution of Gauss sample points maintains the same arrangement for all cells. For example, the first sample point of each cell is located on the same position relative to the vertices for all cells. In consequence, in cases where *dm* is constant during the numerical integration, the weight assigned to the points with the same relative position will be the same. However, in cases where a minimum specified number of points is used to determine the *dm* this does not happen (see Fig. 8).

Table 3. Variation of *dm* in the integration of the stiffness matrix **K**.

dm	d_{max} = 1.0	d_{max} = 1.5	d_{max} = 2.0	d_{max} = 2.5	d_{max} = 3.0	d_{max} = 3.5
Maximum	9.22	13.83	18.44	23.06	27.67	32.28
Average	6.33	9.50	12.67	15.84	19.01	22.18
Minimum	5.39	8.09	10.79	13.49	16.19	18.89
Standard deviation	0.71	1.07	1.42	1.78	2.14	2.50

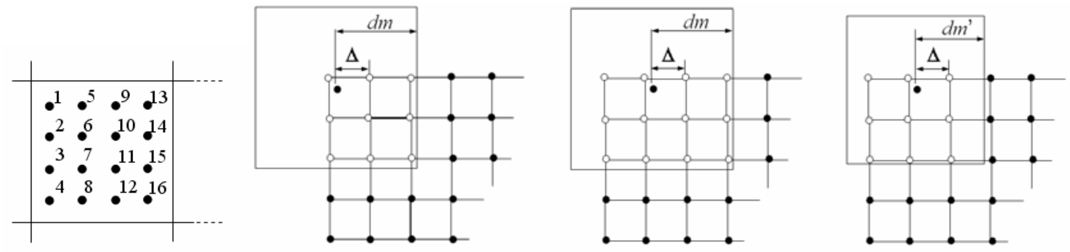

(a) (b) (c) (d)

Figure 8. (a) Sample Gauss points inside of integration cells. (b) Influence domain for the first sample Gauss point in the first cell, and (c) for the 2th cell maintaining *dm* constant, and (d) minimal specified number of points

5. CONCLUSION

This paper presents an analysis of the influence of the parameters related to the EFG method, as well as the validation of the developed program, for a uniform distribution of nodes. This analysis takes in consideration different weight functions, the size *dm* of the influence domain, and the variation of *dm* during the integration for a uniform distribution of nodes. With regard to the tested weight functions we verify that the spline, the Gaussian, and the Exp1 had presented the best results. The advantage to work with the spline functions is that they do not present any parameter of adjustment that must be taken in consideration when using another configuration of points and meshes. The change of the weight function strongly affects the response of the model, and changes in the size of the influence domain lead to coarse variations in the response for the same function. We also verify that the minimum error is associated with a range of *dm* that encompasses a certain amount of points inside of the influence domains. With regard to the changes of *dm* during the integration we verify that even working in this range, the response of the model lost accuracy due to possible changes in weighting nodes inside the influence domain as explained in section 4.3. We also verify that the results for normal stress and displacement fields are better than the response of the shear stress field because we utilize a linear basis in the approach (first-order consistency).

6. REFERENCES

Belytschko, T., Lu, Y.Y. and Gu, L., 1994, "Element-Free Galerkin methods", International Jounal for Numerical Methods in Engineering, Vol. 37, No 2 , pp. 229-256.

Belytschko, T., Krongaunz, Y., Oregan, D. and Fleming, M., 1996, "Meshless Methods: an overview and recent developments", Computer Methods in Applied Mechanics and Engineering, Elsevier, Vol.139, No 1, pp. 3-47.

Dolbow, J. and Belytschko,T, 1998, "An introduction to programming the Meshless Element Free Galerkin Method". Archives of Computational Methods in Engineering, Vol. 5, No 3, pp. 207-241.

Duarte A. C., 1995, "Review of some meshless methods to solve differential equations". Technical Report 95-06 TICAM, University of Texas at Austin.

Liu G. R., 2004, "Mesh Free Methods: moving beyond the finite element method", Ed. CRC Press, Florida,USA, 712 p.

Nayroles, B., Touzot, G. and Villon, P., 1992, "Generalizing the finite element method: diffuse approximation and diffuse elements", Computational Mechanics, Vol. 10, pp. 301-318.

Shuyao, L. and De'an H., 2003, "A study on the weight function of the moving least square approximation in the Local Boundary Integral Equation Method", Acta Mecanica Solida Sinica,Vol. 16, No 3, pp. 276-282.

Timoshenko, S.P. and Goodier, J.N., 1970, "Theory of elasticity", Ed. McGraw Hill, New York, USA, 608 p.

Xiaofei, P., Yim, S. K. and Xiong, Z., 2004, "An Assessment of the Meshless Weighted Least-Squaremethod", Acta Mechanica Solida Sinica, Vol. 17, No. 3, pp. 270-282.

7. RESPONSIBILITY NOTICE

The authors are the only responsible for the printed material included in this paper.